International seminar on ejector/jet-pump technology and applications

Louvain-la-Neuve, Belgium
September 7-9, 2009

Paper No. 06

PREDICTION OF CONDENSATION IN A TWO STAGE STEAM EJECTOR FOR A REFRIGERATION SYSTEM

Giuseppe Grazzini, Adriano Milazzo, Samuele Piazzini
Dipartimento di Energetica – Università di Firenze
Via di S. Marta, 3 – 50139 FIRENZE (ITALIA); +39 055 4796333 – adriano.milazzo@unifi.it

ABSTRACT

An experimental refrigeration system based on a two stage steam ejector was set up in the Thermodynamics and Heat Transfer Laboratory of our Department. The system optimization and realization has been described elsewhere [1].

The primary flow in the first stage is highly supersonic and reaches very low pressure and temperature levels at the nozzle exit. As usual in the technical literature, an ideal gas model was used in the analysis. Therefore, in order to asses the validity of this analysis, verification has to be carried out with respect to real gas behaviour.

High flow speed suggests the establishment of meta-stable conditions in the ejector. In order to understand the actual working condition of our system, an extensive search was made in the literature and several models compared.

Wide agreement exists on the significance of the spinodal curve as a theoretical border to the metastable region. Spinodal curves are derived from the Van der Waals isothermals. These curves were drawn for water, despite the rather scarce availability of thermodynamic data about water at low temperatures.

Some information comes from this analysis and will be used in further optimization of this and other ejector configurations.

NOMENCLATURE

a, b	Constants in Van der Waals Equation
c	Velocity
c_p	Constant pressure specific heat
f	Helmholtz potential
h	Enthalpy
$h_{l\text{-}v}$	Latent heat of vaporization
j, J	Flux
K_B	Boltzmann constant
k	Specific heat ratio
M	Mass flow rate
N	Number of molecules
N_A	Avogadro number
p	Pressure
R	Gas constant
$\mathcal{R}$	Universal gas constant
r	radius
s	Entropy
T	Temperature
v	Specific volume
δ	Reduced density
ρ	Density
σ	Surface tension
τ	Reduced temperature
Ω	Section

Subscripts and superscripts

c	critical point
e	equilibrium
l	liquid
ms	metastable
s	saturation
v	vapour
$*$	critical section or radius

INTRODUCTION

The possibility of working with two-phase flows is one of the reasons for preferring ejector-based systems. This is particularly important when working with water as a refrigerant fluid. However, perfect gas behaviour is often assumed for the working fluid [2,3,4]. This assumption may be useful in order to keep the modelling at a reasonable level of complexity, but some attempts can be made at using results obtained in other technical fields to check the validity of the ideal gas approach, and possibly evolve it toward a more realistic modelling.

When dealing with metastable states, which are very likely to occur in a "fast" device like an ejector, an initial well-established approach relies on "Spinodal" curves [5,6]. These curves will be plotted for water at low pressure and temperature in this paper and will be used as an ultimate boundary for the metastable region. Different tools have been used for example in the analysis of steam turbines. In this field, the metastable boundary is often expressed in terms of "Wilson curve", and the evolution rate of the transformation is explicitly accounted for. The key concept in this case is the nucleation of drops within the expanding vapour, which is ruled by a complex mechanism involving heat and momentum exchange and phase transition.

These concepts will be applied to the experimental refrigeration system that has been set-up in the Thermodynamics and Heat Transfer Laboratory of our Department. This system is based on a two stage steam ejector and was designed by means of a numerical optimization procedure presented in [1]. Ideal gas fluid behaviour was assumed throughout the optimization

process. One of the objective of this paper is to check whether the removal of this assumption would produce significant departures from previous results.

1. SPINODAL CURVES

Spinodal curves can be seen as a consequence of the Van der Waals Theory of liquid-gas phase transition. This theory aimed to account for the non-zero size of molecules and attractive force between them. The Van der Waals equation of state:

$$\left(p+\frac{a}{v^2}\right)(v-b)=RT \tag{1}$$

can be written as:

$$v^3-\left(b+\frac{RT}{p}\right)v^2+\frac{a}{p}v-\frac{ab}{p}=0 \tag{2}$$

showing that, for given p and T values, there can be up to 3 values of v. This happens below the critical point, whose coordinates are related to a, b and R as follows:

$$p_c=\frac{a}{27b^2},\quad v_c=3b,\quad RT_c=\frac{8a}{27b} \tag{3}$$

The shape of the curve below the critical point is far from the equilibrium behaviour of real fluids. All states between the saturated liquid and the saturated vapour curves appear unrealistic. However, it has been shown [5,6,7] that some of these states can actually be reached in metastable conditions. This can be true for the Van der Waals isothermal segments comprised between the saturated liquid curve and the minimum and the saturated vapour curve and the maximum.

On the other hand, in curve segment between the minimum and maximum it is $(\partial p/\partial v)_T>0$, which represents an unstable condition [7]. Therefore, the loci of the minima and maxima on the isothermals mark the boundary between the two metastable areas (on the sides) and the unstable area (in the middle).

Unfortunately, the Van der Waals equation is a poor approximation of the behaviour of real substances. For example, if we calculate the coefficients a, b and R from the conditions (3), the data at lower temperatures turn out to be very far from reality.

Given the interest of the Van der Waals equation as a means to build the spinodal curves, we can try to improve the approximation of equation (2) by adapting coefficients a, b and R at the various temperatures. If the useful zone is that comprised between the saturated liquid and saturated vapour, an initial condition is that the equation should calculate the correct liquid and vapour specific volume at the saturation pressure pertaining to the given temperature. This means:

$$p_s=\frac{RT_s}{(v_l-b)}-\frac{a}{v_l^2}=\frac{RT_s}{(v_v-b)}-\frac{a}{v_v^2}, \tag{4}$$

A third condition can be obtained from the "Maxwell condition" [5], that is the null value of the work for the thermodynamic cycle comprising the Van der Walls isothermal and the constant pressure vaporization. This means that the two areas between the $p = p_s$ horizontal line and the lower and upper part of the S shaped Van der Waals curve must be equal. Hence:

$$\int_{v_l}^{v_v}\left[\frac{RT_s}{(v-b)}-\frac{a}{v^2}-p_s\right]dv=0 \tag{5}$$

By integrating, we have a further condition:

$$RT_s\ln\left(\frac{v_v-b}{v_l-b}\right)=\left(p_s+\frac{a}{v_lv_v}\right)(v_v-v_l) \tag{6}$$

By solving equations (4) and (6) and rearranging them we have

$$\frac{v_l-b}{v_l}\left[\frac{v_v-b}{v_v-v_l}ln\left(\frac{v_v-b}{v_l-b}\right)-1\right]=\frac{2v_v-v_l}{v_l+v_v} \tag{7}$$

which can be solved for b and hence gives $a=\frac{v_l^2v_v^2}{(v_l-b)(v_v+v_l)-v_l^2}p_s$ and $R=\left(p_s+\frac{a}{v_l^2}\right)\frac{(v_l-b)}{T_s}$.

The maxima and minima of these isotherms are given by:

$$0=\frac{dp}{dv}=-\frac{RT}{(v-b)^2}+\frac{2a}{v^3}$$

that is:

$$v^3-\frac{2a}{RT}v^2+\frac{4ab}{RT}v-\frac{2ab^2}{RT}=0 \tag{8}$$

Data for water down to temperatures of – 60°C can be found in [8]. At lower temperatures the values for a, b and R were obtained by extrapolation. From these data we derived the Van der Waals isotherms shown in figure 1 and hence the spinodal curve (in blue) for the metastable vapour phase.

Obviously the isotherms drawn in this way are not representative of the real steam behaviour outside the saturated vapour curve. Moreover, this result must be understood as an ultimate limit for single phase survival. Some other indications will be given in the following sections.

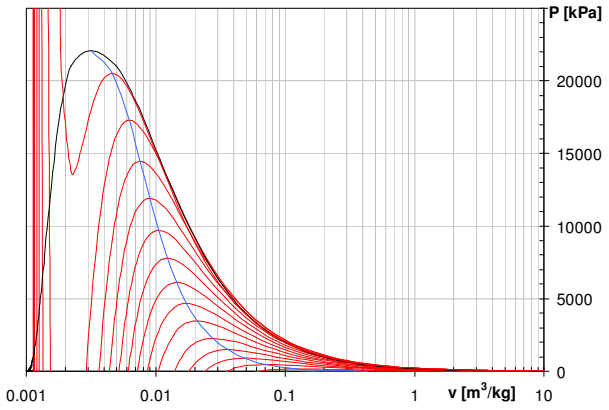

Figure 1 – Spinodal curve for water

2. EXPANSION

Expansion in a nozzle can be modelled assuming the conservation of total enthalpy. In the converging part of the nozzle:

$$c_c^2=c_0^2+2(h_0-h_c) \tag{9}$$

Conservation of mass yields:

$$c_0 = \frac{M v_0}{\Omega_0} = \frac{\Omega_c}{\Omega_0}\frac{v_0}{v_c} c_c \tag{10}$$

Substitution in (9) gives the velocity in the critical section:

$$c_c = [2(h_0 - h_c)]^{1/2}\left(1 - \frac{\Omega_c}{\Omega_0}\frac{v_0}{v_c}\right)^{-1} \tag{11}$$

Usually the critical section is much smaller than the initial on and hence the second term in the rightmost parenthesis is negligible. Critical conditions are found from the maximum of the specific flow rate

$$\left[\frac{\partial(c/v)}{\partial(p/p_0)}\right]_{\Omega_c} = 0 \tag{12}$$

2.1. IDEAL GAS MODEL

In the case of an ideal gas, assuming an isentropic expansion, the specific volume is related to pressure:

$$\frac{v}{v_0} = \left[\frac{p_0}{p}\right]^{1/k} \tag{13}$$

where k is the specific heat ratio. The simplest approach assumes a constant value of k throughout the expansion. This scheme, notwithstanding its minimal refinement, has been extensively used in the literature [2,3,4].
Furthermore, when temperatures below 0°C are reached, it is quite difficult to have c_p and c_v values for water.
For an adiabatic, reversible flow in a fixed horizontal channel

$$c\,dc + v\,dp = 0 \tag{14}$$

Substitution of the specific volume found in (13) allows integration and calculation of the c/v ratio as a function of p.

$$\frac{c}{v} = \sqrt{\frac{2k}{k-1}\frac{p_0}{v_0}\left(\left(\frac{p}{p_0}\right)^{2/k} - \left(\frac{p}{p_0}\right)^{\frac{k+1}{k}}\right)} \tag{15}$$

Zeroing the first derivative of this expression gives the critical conditions:

$$\frac{p^*}{p_0} = \left(\frac{2}{k+1}\right)^{\frac{k}{k-1}};\ c^* = \sqrt{\frac{2kp_0v_0}{k+1}};\ v^* = \left(\frac{k+1}{2}\right)^{\frac{1}{k-1}} v_0 \tag{16}$$

and hence the mass flow rate:

$$M = \Omega_c\sqrt{\left(\frac{2}{k+1}\right)^{\frac{k+1}{k-1}} k\frac{p_0}{v_0}} \tag{17}$$

Once the mass flow rate is known, the pressure in any section Ω can be calculated by solving the equation:

$$\left(\frac{p}{p_0}\right)^{\frac{2}{k}} - \left(\frac{p}{p_0}\right)^{\frac{k+1}{k}} = \frac{2k-1}{2k}\frac{v_0}{p_0}\left(\frac{M}{\Omega}\right)^2 \tag{18}$$

Equation (13) yields the specific volume. Temperature and speed can be calculated from the energy equation.
The nozzle was modelled by a one-dimensional grid of 101 nodes, with node spacing gradually decreasing towards the throat and increasing downstream of it. The same grid has been maintained throughout the paper.
The following data have been assumed:

Initial temperature	T_0	377.15	K
Initial pressure	p_0	116.78	kPa
Constant pressure specific heat	c_p	2059.4	J kg^{-1} K^{-1}
Specific heat ratio	k	1.336	

The nozzle profile is shown in the following diagram:

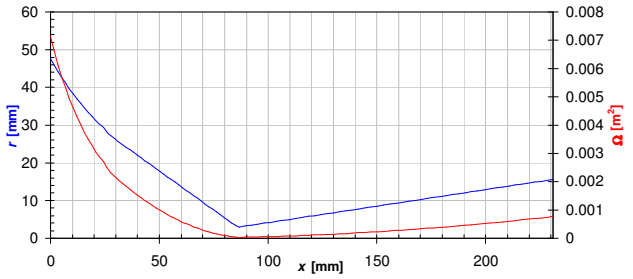

Figure 2 – Nozzle radius r (blue) and section Ω (red)

$\Omega_c = 2.79\cdot10^{-5}$ m^2 being the minimum section, the critical parameters are $p^* = 62.97$ kPa and $c^* = 441$ m/s. Mass flow rate turns out to be $M = 5.32\cdot10^{-3}$ kg/s.
The results in terms of pressure, velocity, Mach number and temperature along the nozzle are shown in figure 4 (blue curve).
These results are relatively insensitive to assumed c_p and k values. A moderate variation in the exit temperature is found when these values are varied over their complete range. Therefore no attempt was made to introduce the variability of these parameters in the ideal gas model.
The ideal gas expansion was drawn on a pv diagram (figure 4) together with the spinodal curve. The latter ends at a quite high pressure value, due to the lack of data at temperatures below -60°C.
Clearly, the expansion diverges from the spinodal curve. Hence condensation appears unlikely, especially when entropy increase due to irreversibility moves the curve to the right. This result, however, will be partly contradicted in the following sections.

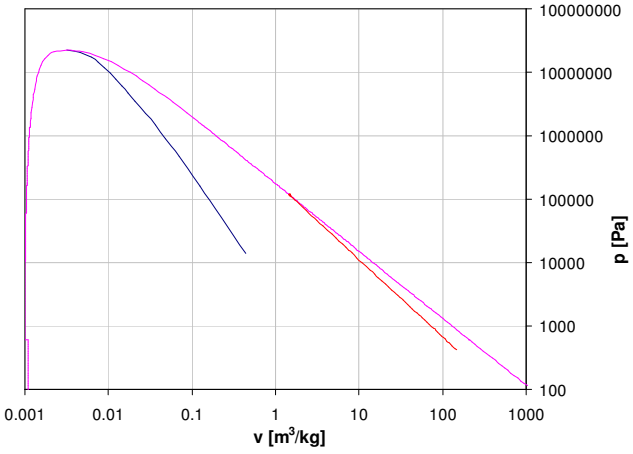

Figure 3 – Comparison between ideal gas expansion (red) and spinodal curve (blue)

2.2. SATURATED VAPOUR MODEL

An opposite, but equally extreme simplification would be to assume that the fluid, within the two phase zone, is in thermodynamic equilibrium. This would completely change the fluid behaviour and does represent a significant boundary condition, because it gives the maximum amount of water which can be condensed inside the nozzle.
In this case, the pressure/volume relation can no longer be expressed in a closed form. The constancy of entropy s at any temperature T yields a vapour mass fraction:

$$x = \frac{s - s_l(T)}{s_v(T) - s_l(T)} \tag{19}$$

From x, all the fluid properties can be found. Given the expected low temperature at nozzle exit, saturated liquid and vapour data have been collected from [8]. Therefore, we can draw a constant entropy line on the phase diagram and calculate the c/v ratio along it. Again, the maximum value of this ratio must coincide with the minimum section of the nozzle.
Given the same inlet conditions used in the perfect gas model, the critical values for saturated vapour are:

p^* = 67.56 kPa and c^* = 428 m/s.

Mass flow rate is $M = 5.06 \cdot 10^{-3}$ kg/s.
Once mass flow rate is known, we may calculate the conditions in each section by solving the continuity and energy equations iteratively. Results are shown in figure 4 (red curve).
Exit velocity is increased by the slight specific volume decrease due to condensation. Exit vapour mass fraction is 0.79. The most noticeable feature of these results is the higher exit temperature, 271.5 K against 118.3 K that was found with the ideal gas model. This is clearly due to the condensation, which gives a significant energy contribution even if the condensed liquid is a rather small percentage.
Another useful result from this model is the vapour mass fraction along the expansion. In the present case, its minimum value, at nozzle exit, is x = 0.79. This value is an index of the maximum amount of liquid water formed within the nozzle.

2.3. METASTABLE VAPOUR MODEL

A more realistic model should include the significant deviations of the real fluid from ideal gas behaviour. Moreover, it should take into consideration the fact that thermodynamic equilibrium can hardly be established in the short timeframe of the expansion in a supersonic nozzle. The most reliable description of the metastable behaviour of steam available in the literature is reported in [9]. In the cited paper a large collection of experimental data is summarized in an analytical expression via multiparameter fitting allowing for a very accurate estimation of the thermodynamic properties. Data available for the metastable field are included in a simplified formulation specific for the gas phase which we employed for the present analysis. It is important to underline that this is a physics-based real-gas model but condensation is not included. Indeed, as will be shown later, we extended the application of the formulation far beyond the limit where condensation is expected.
All relevant parameters are written in terms of the Helmholtz potential,

$$\frac{f}{RT} = \phi^0(\delta,\tau) + \phi^r(\delta,\tau) \tag{20}$$

which in turn is written as a function of reduced density and temperature:

$$\delta = \frac{\rho}{\rho_c} \qquad \tau = \frac{T_c}{T}$$

where ρ_c = 322 kg/m^3 and T_c = 647.096 K are water critical parameters and R = 461.52 J kg^{-1} K^{-1} is the gas constant for water.

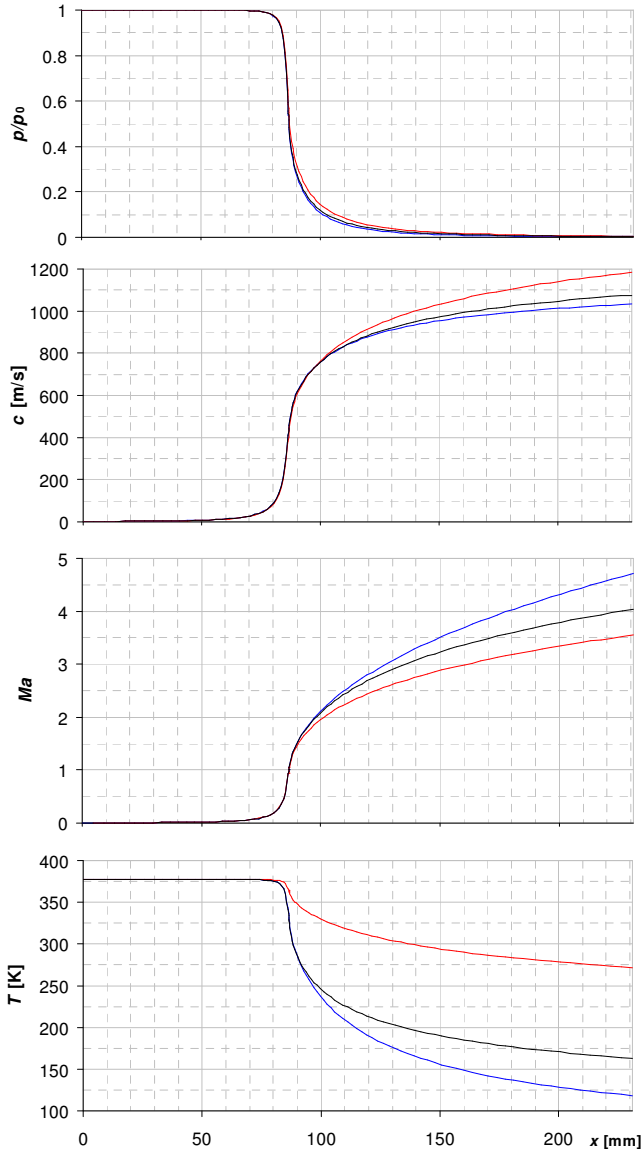

Figure 4 – Comparison of results:
blue line = ideal gas
red line = saturated vapour
black line = metastable vapour

The non-dimensional Helmholtz potential has two contributions: ϕ^0 (ideal part) and ϕ^r (residual part), the latter accounting for the real gas behaviour. The

complete expressions for these contributions are given in [9] along with all required parameters.
Once ϕ^0 and ϕ^r are computed, the following relations:

$$\frac{p}{\rho RT} = 1 + \delta\phi_\delta^r$$
$$\frac{h}{RT} = 1 + \delta\phi_\delta^r + \tau\left(\phi_\tau^0 + \phi_\tau^r\right) \quad (21)$$
$$\frac{s}{R} = \tau\left(\phi_\tau^0 + \phi_\tau^r\right) - \phi^0 - \phi^r$$

return the values of the needed properties, ϕ_δ and ϕ_τ being the derivatives of ϕ with respect to δ and τ.
For what concerns the solution of the nozzle expansion problem we implemented a procedure based on the conservation equations for mass, momentum and energy similar to the one described in sections 2 and 2.1 but without the shortcuts provided by the ideal gas assumption.
The results are shown in figure 4 (black curve). As expected, these results lie between those of the two simpler models.
Differences appear rather small in terms of pressure. However, taking as a reference the pressure p_{ms} calculated by metastable model, it may be seen that the ideal gas model (blue line) underestimates the nozzle exit pressure and the saturated vapour model overestimates it by about 40% (figure 5).

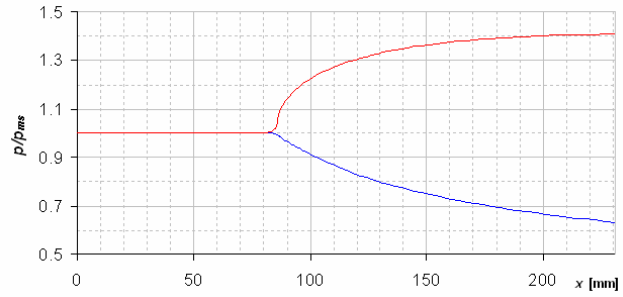

Figure 5 – Pressure according to saturated vapour (red line) and ideal gas (blue line) models divided by the metastable model result

Velocity and temperature values resulting from the metastable vapour model are closer to those of the ideal gas model.

3. NUCLEATION

It is now interesting to estimate whether and under which condition condensation takes place.
Real phase change occurs under non-equilibrium conditions. The initiation of condensation processes is achieved after at least a portion of the vapour phase has been subcooled below its saturation temperature. The subcooling level depends on the initial state and the expansion rate, and can reach several tens of degrees.
Homogeneous nucleation is the process of droplet formation within a subcooled vapour. This mechanism prevails over heterogeneous nucleation, i.e. nucleation on solid walls (or dispersed solid particles), the heat transfer at walls being too low in order to have a relevant condensation on them.

In Classical Nucleation Theory (CNT) the vapour phase is modelled as an ideal gas and the liquid phase is assumed to be incompressible.
The liquid in a drop with radius r immersed in a vapour phase at pressure p_v has a higher pressure:

$$p_l = p_v + \frac{2\sigma}{r} \quad (22)$$

due to the surface tension σ. The latter can be calculated according to [10] as:

$$\sigma = 235.8\, t^{1.256}\,(1 - 0.625\, t) \quad (23)$$

with $t = 1 - T / T_c$
At thermodynamic equilibrium, the chemical potential of the liquid and vapour phases must be equal. This gives a relation between the two pressure values in the form:

$$p_v = p_s(T_v)\, exp\left\{\frac{v_l\left[p_l - p_s(T_v)\right]}{RT_v}\right\} \quad (24)$$

where $p_s(T_v)$ is the saturation pressure at vapour temperature T_v and p_l is found from (22). This relation can be used to find the equilibrium value for the droplet radius. Molecule clusters with radial size below the equilibrium value are unstable, rapidly growing and then shrinking. When the radius of a cluster reaches r^* (critical radius), the cluster undergoes a phase transition and becomes a droplet (sub-micron scale). Due to phase-change, droplets release heat into the surrounding gas phase, with consequent reduction of subcooling and pressure recovery. The two-phase system evolves towards the restoration of an equilibrium state.
The critical radius was calculated throughout the expansion using the pressure and temperature values calculated by the metastable vapour model by the CNT relation [11]:

$$r^* = \frac{2\sigma T_s}{\rho_l h_{l-v}(T_s - T_v)} \quad (25)$$

h_{l-v} being the latent heat of evaporation.
The result is shown in figure 6. The critical radius decreases steadily along the converging part of the nozzle and falls to very low values in the nozzle throat. Within the gas phase smaller clusters are by far more abundant; this implies that, along with the reduction of the critical radius, nucleation becomes more likely. Equation (25) shows clearly the dependence of the critical radius on the subcooling level, i.e. the difference between saturation and local temperatures.

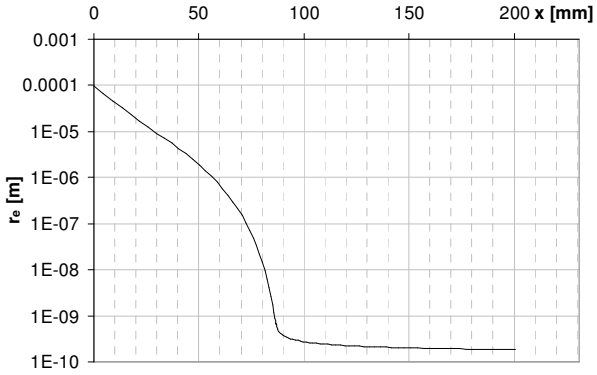

Figure 6 – Critical droplet radius

Therefore, we can deduce that our system is prone to condensation and the nozzle throat is the critical section with respect to nucleation.

Once nucleation conditions are established, we need to estimate the number of droplets actually formed out of the vapour phase. Given the number of droplets and their average size, it is possible to compute the amount of liquid phase in the mixture, hence a two-phase approach similar to the one described in section 2.2 is viable for the solution of the nozzle flow.

Again, Classical Nucleation Theory provides us an expression for the nucleation rate (J), that is the number of condensed nuclei formed per unit time and unit volume of fluid. For instance, newly formed nuclei have critical radius: different sizes are statistically irrelevant. Expressions of J as a function of the vapour conditions may be found for example in [7].

Here a formulation taken from [11] accounting for the rate of formation of droplets of the critical size was used:

$$J^* = \frac{1}{1+\eta}\left(\frac{2\sigma}{\pi m^3}\right)^{1/2}\frac{\rho_v^2}{\rho_l}\exp\left[-\frac{4\pi(r^*)^2\sigma}{3K_B T_v}\right] \quad (26)$$

where m is the mass of one molecule (i.e. the molar mass divided by the Avogadro number N_A), $K_B = \mathcal{R} / N_A$ is the Boltzmann constant and η is a correction factor introduced into the CNT formulation to improve the agreement with experimental data:

$$\eta = 2\frac{k-1}{k+1}\frac{h_{l-v}}{RT_v}\left(\frac{h_{l-v}}{RT_v}-\frac{1}{2}\right) \quad (27)$$

Clearly, nucleation rate J^* has a very low value when homogeneous nucleation is unlikely and jumps to very high values once it becomes likely. The exponential form amplifies the steep change of critical size seen in figure 6.

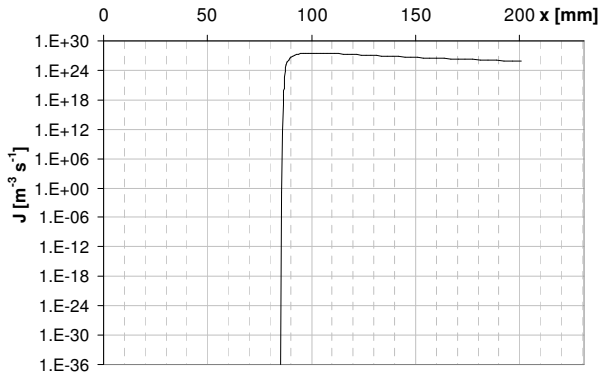

Figure 7 – Nucleation rate

The value of J^* was calculated along the whole nozzle. Results, shown in figure 7, confirms nucleation occurrence in the nozzle throat.

4. CONCLUSIONS

The results of the different models applied to the nozzle of our experimental apparatus prompt the following remarks:

- The spinodal curve can be seen as the ultimate limit for subcooled vapour existence, but in the present case it gives quite misleading results, as it is very far from the expansion curve and yet condensation does occur as can be seen with more accurate analysis.
- The ideal gas schematization is simple and efficient (for example it can be easily modified to account for friction loss), but its results appear to be very far from reality in the case at hand.
- The equilibrium data for saturated values can be used within a simple nozzle model in order to have an upper limit for the amount of liquid formed along the expansion.
- The IAPWS gas equation of state is the most reliable fluid description and can be taken as a reference. Even if rather complex, it can be easily implemented in a simple one-dimensional model giving stable results.
- An ejector working with saturated or slightly superheated vapour, as the one adopted in our experimental refrigeration system, is prone to homogeneous nucleation in the nozzle throat.

All these indications will be used in subsequent work on our refrigeration system, which will include a redesign of the primary nozzle accounting for homogeneous nucleation.

REFERENCES

[1] Grazzini G. and Rocchetti A.: Numerical optimisation of a two-stage ejector refrigeration plant, Int. J. of Refrigeration **25** (2002), 621–633.

[2] Eames I.W.: A new prescription for the design of supersonic jet-pumps: the constant rate of momentum change method, Applied Thermal Engineering **22** (2002), 121-131.

[3] Hallo L., Champoussin J.C., Vignon J.M. and Guerrassi N.: Ejecteurs frigorifiques supersoniques - Modélisation de leurs performances, Revue Générale de Thermique **375-376** (1993) 166-171

[4] Yapici R. and Ersoy H.K.: Performance characterstics of the ejsctor refrigeration system based on the constant area ejector flow model, Energy Conversion and Management **46** (2005) 3117-3135

[5] Lock G. S. H.: Latent Heat Transfer – An introduction to fundamentals, Oxford Science, 1996.

[6] Bejan A.: Advanced Engineering Thermodynamics, John Wiley & Sons, 1988.

[7] V. P. Carey, Liquid-Vapor Phase Change Phenomena, Taylor & Francis, 1992.

[8] 1997 ASHRAE Handbook Fundamental.

[9] Wagner W. and Pruβ A.: The IAPWS formulation 1995 for the thermodynamic properties of ordinary water substance for general and scientific use, J. Phys. Chem. Ref. Data **31** (2002), 387-535.

[10] IAPWS Release on Surface Tension of Ordinary Water Substance, Secretary of IAPWS, http://www.iapws.org/relguide/surf.pdf.

[11] Kermani M.J. and Gerber A.G.: A general formula for the evaluation of thermodynamic and aerodynamic losses in nucleating steam flow, Int. J. of Heat and Mass Transfer **46** (2003) 3265–3278.